

Proposal for the J-PARC 30-GeV Proton Synchrotron:
 ${}^3_{\Lambda}\text{H}$ and ${}^4_{\Lambda}\text{H}$ mesonic weak decay lifetime
measurement with ${}^{3,4}\text{He}(\text{K}^-, \pi^0){}^3,4_{\Lambda}\text{H}$ reaction

H. Asano¹, X. Chen⁴, A. Clozza⁶, C. Curceanu⁶, R. Del Grande⁶, C. Guaraldo⁶, C. Han^{4,1}, T. Hashimoto³, M. Iliescu⁶, K. Itahashi¹, M. Iwasaki¹, Y. Ma¹, M. Miliucci⁶, S. Okada¹, H. Ota¹, K. Piscicchia^{6,8}, F. Sakuma¹, M. Sato², A. Scordo⁶, D. Sirghi^{6,7}, F. Sirghi^{6,7}, K. Tanida³, T. Yamaga¹, X. Yuan⁴, P. Zhang⁴, Y. Zhang⁴, H. Zhang⁵

¹RIKEN, Wako, 351-0198, Japan

²High Energy Accelerator Research Organization (KEK), Tsukuba, 305-0801, Japan

³Japan Atomic Energy Agency, Ibaraki 319-1195, Japan

⁴Institute of Modern Physics, Gansu 730000, China

⁵School of Nuclear Science and Technology, Lanzhou University, Gansu 730000, China

⁶Laboratori Nazionali di Frascati dell INFN, I-00044 Frascati, Italy

⁷Horia Hulubei National Institute of Physics and Nuclear Engineering (IFIN-HH), Magurele, Romania

⁸CENTRO FERMI - Museo Storico della Fisica e Centro Studi e Ricerche "Enrico Fermi", 00184 Rome, Italy

Executive Summary

Three recent heavy ion experiments (HypHI, STAR and ALICE) announced surprisingly short lifetime for ${}^3_{\Lambda}\text{H}$ mesonic weak decay (MWD), which is difficult to interpret given the fact that ${}^3_{\Lambda}\text{H}$ is a very loosely bound system. It will be very interesting to study this issue with a different experimental approach. We propose a direct measurement for ${}^3_{\Lambda}\text{H}$ hypernucleus MWD lifetime with $\sim 20\%$ resolution; ${}^4_{\Lambda}\text{H}$ hypernucleus lifetime will also be measured as a feasibility test for our experimental approach. The major parameters of this experiment are summarized below:

Reaction	: ${}^{3,4}\text{He}(\text{K}^-, \pi^0){}^3,4_{\Lambda}\text{H}$ reaction
Secondary beam	: 1 GeV/c K^-
Beamline	: K1.8BR
Target	: liquid ${}^3\text{He}$ and ${}^4\text{He}$
Detector	: Cylindrical Detector System (CDS) and PbF_2 γ -ray calorimeter
Beam time	: 3 days for detector commissioning
	: 50 kW \times 5 weeks for production run (1 week for ${}^4_{\Lambda}\text{H}$; 4 weeks for ${}^3_{\Lambda}\text{H}$)

Contents

1	Introduction and physics motivation	3
2	Production method	4
3	Production cross section estimation for ${}^{3,4}\text{He}(\text{K}^-, \pi^0){}_{\Lambda}{}^{3,4}\text{H}$ process	7
4	Experimental setup	8
4.1	γ -ray calorimeter	8
4.2	π^- tracker	11
5	Performance estimation	12
5.1	${}_{\Lambda}{}^{3,4}\text{H}$ yield estimation	12
5.2	Background processes and simulation study	12
5.3	Analysis procedure	13
6	Proposal timeline	15
6.1	Liquid ${}^3\text{He}$ target modification	15
6.2	PbF_2 calorimeter construction and commissioning	15
7	Beam time request	16
A	${}_{\Lambda}{}^3\text{H}$ stopping time estimation	18
B	Background Survey	18

1 Introduction and physics motivation

As a very loosely bound system, Hypertriton(${}^3_{\Lambda}\text{H}$, $B_{\Lambda}=130\pm 50$ keV[1]) is expected to possess a similar lifetime as free Λ hyperon ($\tau = 263.2\pm 2.0$ ps). For instance, high precision few-body calculation shows that Λ hyperon is separated by ~ 10 fm from np-pair(deuteron) inside ${}^3_{\Lambda}\text{H}$ [2]. However, three heavy ion experiments(STAR[3], HypHI[4] and ALICE[5]) found surprisingly short lifetime for ${}^3_{\Lambda}\text{H}$ in their measurements. This situation is summarized in Table1.

Collaboration	Experimental method	${}^3_{\Lambda}\text{H}$ lifetime [ps]	Release date
STAR	Au collider	$142^{+24}_{-21}(\text{stat.})\pm 29(\text{syst.})$	2018
ALICE	Pb collider	$181^{+54}_{-39}(\text{stat.})\pm 33(\text{syst.})$	2016
HypHI	fixed target	$183^{+42}_{-32}(\text{stat.})\pm 37(\text{syst.})$	2013

Table 1: Summary of recent measurements on ${}^3_{\Lambda}\text{H}$ lifetime.

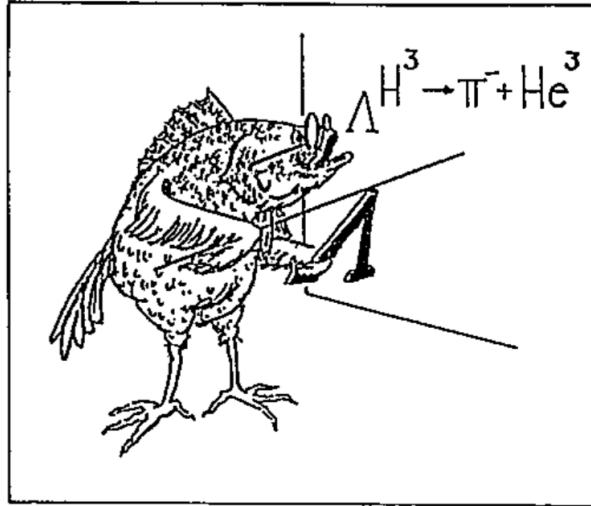


Figure 1: Neither fish nor fowl?[6]

This puzzling situation can be illustrated with Fig.1[6]. In order to shed light on this puzzling issue, we propose to measure ${}^3_{\Lambda}\text{H}$ mesonic weak decay lifetime(${}^3_{\Lambda}\text{H} \rightarrow {}^3\text{He} + \pi^-$) with ${}^3\text{He}(K^-, \pi^0){}^3_{\Lambda}\text{H}$ production reaction. The advantage of this approach is that it allows us to carry out a direct lifetime measurement, which is different from the heavy ion experiments listed above. Data analysis technique is also established during previous KEK weak decay experiments [7][8]. On the other hand, the involvement of π^0 detection makes the reconstruction of hypernuclear ground state with missing mass method very difficult. Our solution is to construct a hadron blind γ -ray calorimeter to tag high energy π^0 events in very forward angle, which corresponds to Λ hyperon production with small recoil momentum. The yield of ${}^3_{\Lambda}\text{H}$ hypernucleus can be enhanced by this event selection condition and result in a relatively good signal to background ratio. The momentum of π^- emitted from ${}^3_{\Lambda}\text{H}$ mesonic weak decay at rest will be mono-chromatically distributed around 114.3 MeV/c because there is only one quantum state for this decay channel. We can identify the ${}^3_{\Lambda}\text{H}$ events by selecting this peak on the delayed π^-

momentum spectrum. The background suppression can be achieved by subtracting the time distribution of the neighboring π^- in momentum spectrum as described in [8].

The same idea can be applied to the ${}^4_{\Lambda}\text{H}$ hypernucleus production and its mesonic weak decay measurement because it shares the same experimental setup except the target material. The ${}^4_{\Lambda}\text{H}$ MWD lifetime has been measured by [8] with $(\text{K}^-_{\text{stopped}}, \pi^0)$ reaction, which will be used as a reference channel to test the performance of our approach.

2 Production method

With a simple phenomenological model, the production of Λ hypernucleus can be treated as a two-step process. First, a Λ hyperon is generated by one of the reactions listed in Fig.2; then the Λ hyperon has to be combined with the rest of nucleus described by a parameter called *sticking probability*. Qualitatively, Λ hyperon with smaller recoil momentum has larger *sticking probability*, which can be used as a guideline for hypernucleus production estimation. This argument is particularly true for *s-shell* hypernucleus because there is only one bound state for Λ hyperon in *s-orbit* and any $\Delta p \geq 200$ MeV/c reaction will cause $\Delta l = 1$ transition. Therefore, we plan to employ ${}^3,4\text{He}(\text{K}^-, \pi^0){}^3,4_{\Lambda}\text{H}$ reaction to populate ${}^3,4_{\Lambda}\text{H}$ for their lifetime measurements because of the small recoil momentum among all three production channels.

In an ideal experimental setup, one can set the K^- beam momentum to be ~ 0.5 GeV/c because the populated Λ hyperon will have no recoil momentum, which is often cited as *magic momentum*. However, it is difficult to prepare K^- beam with such a low momentum because of the K^- decay during transportation. In addition, the Λ hyperon production cross section is relatively low at this K^- beam momentum. A more common choice for Λ hypernucleus production with K^- beam is $p_{\text{K}^-} \geq 0.75$ GeV/c. The current K^- intensity at J-PARC K1.8BR as a function of beam momentum is given in Fig.3[9]. On the other hand, hyperon production cross section for $p(\text{K}^-, \pi)\Lambda(\Sigma)$ elementary process as a function of K^- beam momentum when the projectile π meson comes out at 0 degree is given Fig.4[10]. By combining the K^- beam intensity and hyperon production cross section, a *figure of merit* can be obtained as shown in Fig.5. Taking into account the Λ to Σ ratio and Λ hyperon recoil momentum, our best choice is to perform the experiment at $p_{\text{K}^-} \sim 1$ GeV/c, which is used through out this proposal.

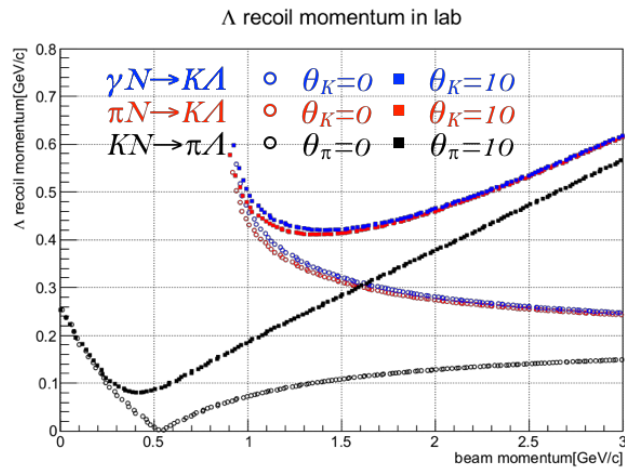


Figure 2: Recoil momentum of Λ hyperon from three different production method; $p(K^-, \pi^0)\Lambda$ reaction has the lowest recoil momentum.

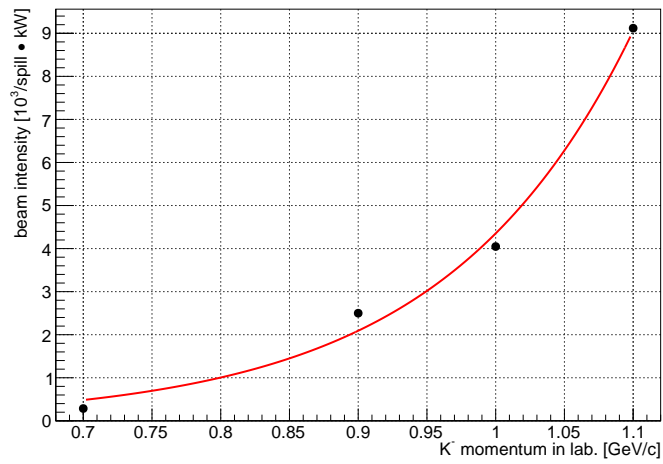


Figure 3: K^- beam intensity at K1.8BR beam line of J-PARC.

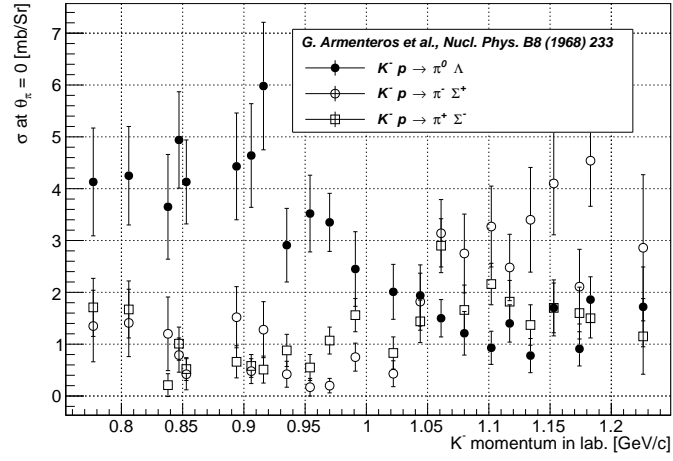


Figure 4: Production cross section for $p(K^-, \pi)\Lambda, \Sigma$ reaction[10].

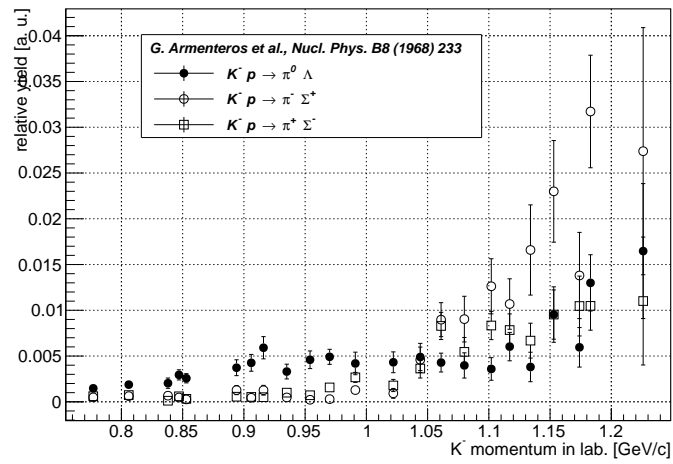


Figure 5: Figure of merit by combining K^- beam intensity and production cross section.

3 Production cross section estimation for ${}^3,4\text{He}(\text{K}^-, \pi^0)_{\Lambda}{}^3,4\text{H}$ process

The production cross section data for ${}^3,4\text{He}(\text{K}^-, \pi^0)_{\Lambda}{}^3,4\text{H}$ process at $p_{K^-}=1.0\text{GeV}/c$ is not available. We will rely on a recent theoretical calculation as shown in Fig.6[11]. Quasi-free Λ hyperon production, which is the most dominant background, is estimated to be ~ 10 times more than hypertriton yield in the forward region. Because these Λ hyperons decay in-flight, the π^- momentum will be distributed between $80 \sim 140\text{MeV}/c$. So that the actual S/N ratio for π^- of $114\text{MeV}/c$ signal region will be much better than $1/10$. A GEANT4 based evaluation will be given in the Section 5 of this proposal. The production cross section of ${}^4_{\Lambda}\text{H}$ is assumed to be three times of ${}^3_{\Lambda}\text{H}$.

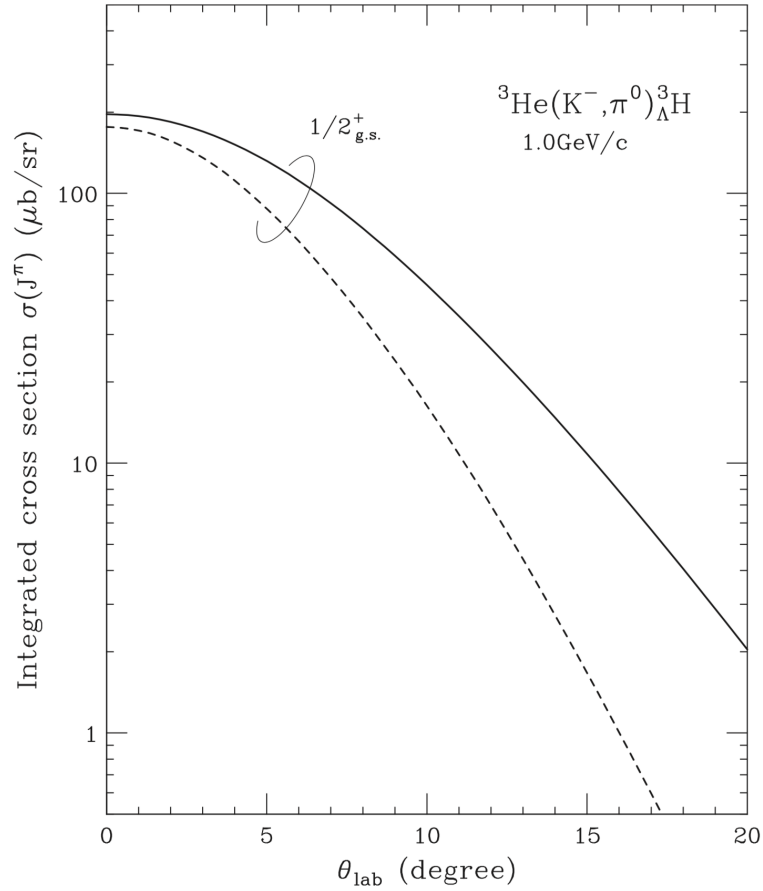


Figure 6: Calculated production cross section for ${}^3\text{He}(\text{K}^-, \pi^0)_{\Lambda}{}^3\text{H}$ reaction at $1\text{ GeV}/c$. [11]

4 Experimental setup

The experimental concept is shown in Fig.7. A Cylindrical Detector System(CDS) used in J-PARC E15/E31 experiment is employed to capture the delayed π^- as a weak decay product from ${}^3_{\Lambda}H$ hypernuclei[12]; a calorimeter is installed in the very forward region to tag fast π^0 meson along ~ 0 degree, which corresponds to small recoil momentum of Λ hyperon. Such a selection will improve the ratio between ${}^3_{\Lambda}H$ and quasi-free Λ and Σ background. In the rest of this section, we will present the details of each detector component.

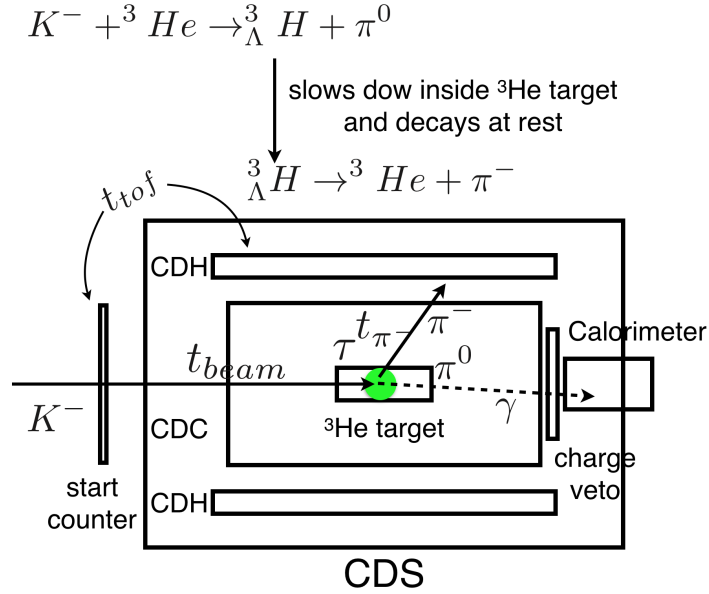


Figure 7: Schematic view of the experimental setup; Cylindrical Detector System(CDS) is used to capture delayed π^- particle from ${}^3_{\Lambda}H$ weak decay; high-energy γ rays ($E_{\gamma} \geq 600$ MeV) are tagged with PbF_2 calorimeter.

4.1 γ -ray calorimeter

The most challenging task for the ${}^3_{\Lambda}H$ production with (K^-, π^0) method is to identify the ground state of ${}^3_{\Lambda}H$ hypernuclei, which involves the detection of π^0 particle. The outgoing π^0 decays into two γ rays almost immediately. The fast π^0 at the forward scattering angle boosts the decayed γ rays more forward than the slow π^0 events as illustrated in Fig.8. For π^0 with momentum of ~ 0.9 GeV/c and $\theta_{\pi^0}=0$, the opening angle between decayed γ rays is centered at $\pm 7^\circ$. By covering the $0^\circ \sim 7^\circ$ region of polar angle, we can tag the γ ray decayed from π^0 with higher energies.

One can expect very high background rate from the unreacted beam hitting on the forward γ -ray calorimeter. After searching for available materials available on the market, we decide to use PbF_2 crystal as Cherenkov based γ -ray calorimeter. Table 2 summarizes related property of PbF_2 crystal. As shown in Fig.9, the PbF_2 crystals have a nice separation between pion and electron (and also γ) because of Cherenkov radiation mechanism [13]. As demonstrated by Fig.10, the PbF_2 crystal possesses good radiation hardness. For instance, an average of ~ 240 MeV will be deposited into $2.5 \times 2.5 \times 14$ cm³ PbF_2 crystal by K^- beam particle of 1 GeV/c according to GEANT4 simulation. Assuming an intensity of 10^6 /s, including π^- contamination, 4 Gy/day of radiation dose can be expected. The accumulated

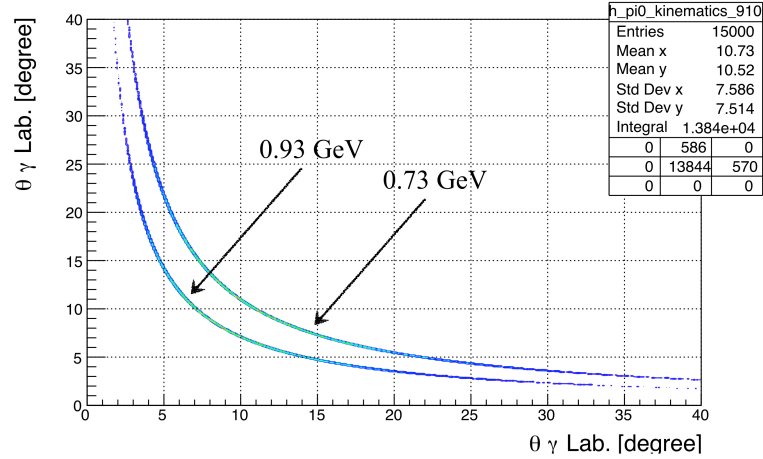


Figure 8: Angular correlation of γ rays decayed from π^0 with different momentum; upper curve is for $p_{\pi^0} = 0.73$ GeV/c; lower curve is for $p_{\pi^0} = 0.93$ GeV/c.

radiation dose during one month of data taking will be ~ 100 Gy, which will not have any significant performance degradation according to Fig.10 [13]. In addition, it is found that the PbF_2 can be recovered from radiation damage by exposed to light source of 365 nm wave length [13]. PbF_2 crystal also generates very fast signal with duration of ~ 20 ns because of its Cherenkov nature.

In the present design, we will use a 5 by 5 (25 pieces) PbF_2 segments with $2.5 \times 2.5 \times 14$ cm³ dimension, which costs ~ 1 k USD per crystal. Total budget including photon sensor and readout electronics is ~ 50 k USD. Our funding application was approved in 2017 and the construction of γ -ray calorimeter is in progress.

Crystal	Radiation length	Moliere radius	Density	Cost ¹
PbF_2	0.93 cm	2.22 cm	7.77 g/cm ³	12 USD/cc

Table 2: Summary of PbF_2 crystal property.

¹Unofficial quotation from SIC, CAS, Shanghai, China.

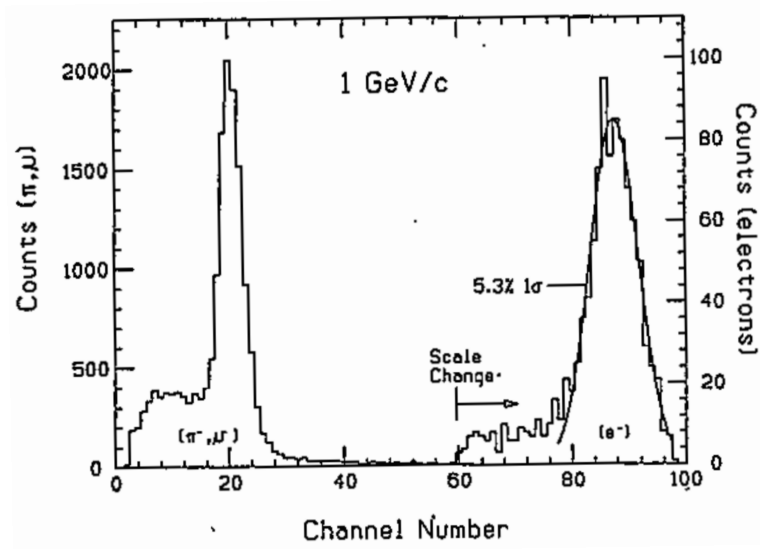


Figure 9: Light yield for 1 GeV/c pion and electron [13].

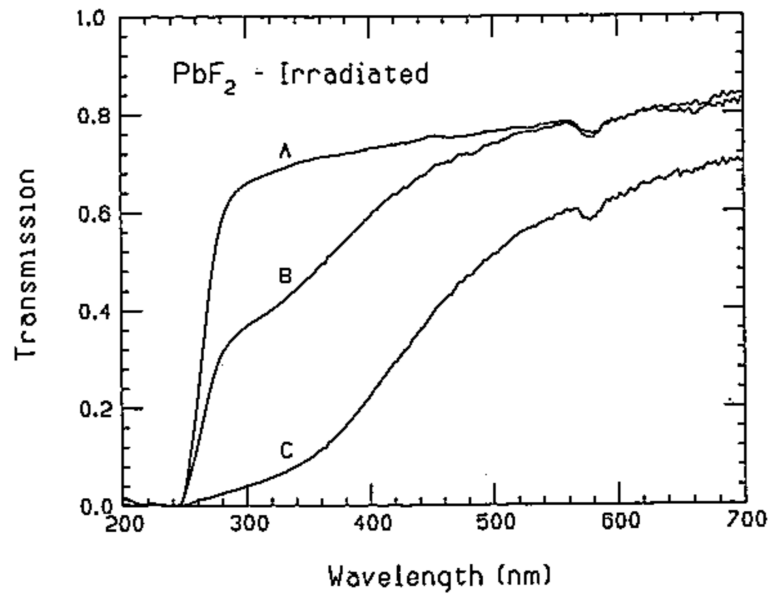


Figure 10: Effects of radiation dose on PbF_2 transmission: (A) is before radiation; (B) after 3×10^5 rad of neutron and 1×10^5 rad of γ rays; (C) after 3×10^6 rad of neutrons and 1×10^6 rad of γ rays [13].

4.2 π^- tracker

The produced ${}^3_{}{}^4_\Lambda\text{H}$ hypernucleus partially ($\sim 25\%$ and $\sim 50\%$, respectively) decays into ${}^3,4\text{He}$ and π^- , whose lifetime will be derived by the proposed experiment. If the ${}^3,4_\Lambda\text{H}$ hypernuclei decay at rest, the π^- meson will have a well defined momentum of 114.3 and 133 MeV/c, respectively. The actual π^- distribution will be smeared out slightly because of the ${}^3,4_\Lambda\text{H}$ in-flight decay. As can be seen in Appendix A, the recoiling ${}^3,4_\Lambda\text{H}$ will be stopped within ~ 200 ps (or, ~ 1 mm) due to stopping effect inside the target. As one can easily estimate, for ${}^3,4_\Lambda\text{H}$ hypernuclei, the in-flight decay effect for π^- is very limited because of the slow velocity of the recoiling mother particle. This observation is confirmed by our simulation in Section 5.

The proposed experiment is, in principle, a semi-inclusive measurement. The momentum resolution for π^- is the key factor for a successful identification for the production of ${}^3,4_\Lambda\text{H}$ hypernuclei. We will use Cylindrical Detector System (CDS) originally designed for J-PARC E15 experiment for its demonstrated good performance. The CDS consists of a solenoid magnet, Cylindrical Drift Chamber (CDC) and a hodoscope made of plastic scintillator (CDH). For details, please refer to [12]. The momentum resolution of CDS is given in Fig.11, which is obtained with 0.7 T magnetic field[14]. The transverse momentum resolution for the interested region ($p_{\pi^-}=114$ MeV/c) is as good as $\sim 1.5\%$. For π^- momentum lower than 110 MeV/c, the resolution becomes worse rapidly because of the energy loss of charged π^- inside target materials. This can be improved by correcting for the energy loss inside the CDS. According to our simulation, a total momentum resolution of $\sim 2\%$ can be achieved without major modification of the current setup.

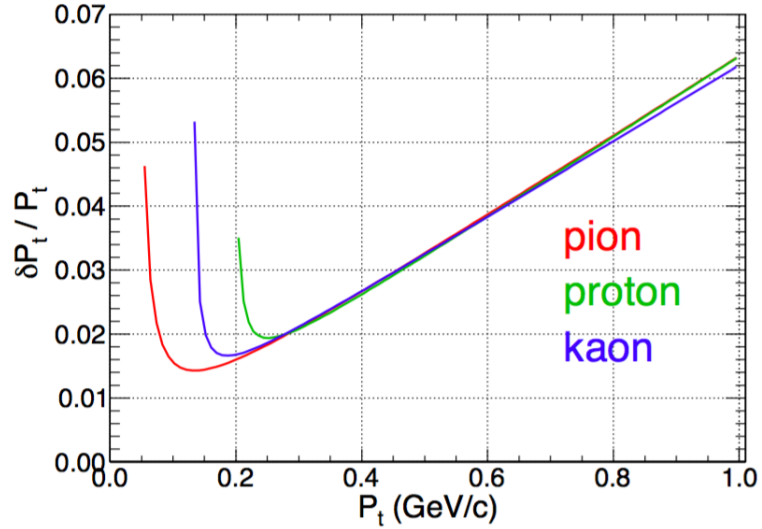


Figure 11: Momentum resolution of CDS [12].

5 Performance estimation

5.1 ${}^3_{\Lambda}\text{H}$ yield estimation

The yield of ${}^3_{\Lambda}\text{H}$ has been summarized in Table 3. The location of γ -ray calorimeter plays important role in the signal yield estimation because of the π^0 acceptance strongly depends on the distance between calorimeter and target. However, one can not leave the calorimeter very close to the target because of the large material budget of PbF_2 crystal causes serious contamination inside the CDS spectrometer. In the current estimation, we suppose the calorimeter is installed 70cm down stream from the target center.

Parameter	Value	Yield
${}^3_{\Lambda}\text{H}$ integrated cross section	$\bar{\sigma}_{0\sim 20} = 0.0126\text{mb}$	
${}^3\text{He}$ target(10 cm)	$A = \frac{1}{3} \times 0.08\text{g/cm}^3 \times 10\text{cm} \times 6.02 \times 10^{23} = 1.6 \times 10^{23}/\text{cm}^2$	
K^- at 1 GeV/c(4 weeks)	$B = 2 \times 10^5 / 5.2\text{s} \times 3600 \times 24 \times 28 = 9 \times 10^{10}$	
Total yield	$\bar{\sigma}_{0\sim 20} \times A \times B$	1.8×10^5
${}^3_{\Lambda}\text{H} \rightarrow \pi^-$ branching ratio	0.25	4.5×10^4
Beam acceptance & DAQ eff.	~ 0.5	2.2×10^4
π^0 & π^- acceptance & event selection	6%	1.3×10^3

Table 3: ${}^3_{\Lambda}\text{H}$ Yield estimation.

As can be read from Table 3, $\sim 1.3\text{k}$ ${}^3_{\Lambda}\text{H}$ events will be collected with 4 weeks beam time. If we assume $\sigma_{{}^3_{\Lambda}\text{H}}/\sigma_{{}^4_{\Lambda}\text{H}} = 1/3$ and taking into account the factor of 2 from two-body π^- decay branching ratio between ${}^4_{\Lambda}\text{H}$ (b.r. = 50%) and ${}^3_{\Lambda}\text{H}$ (b.r.=25%), one can expect 1.8k events from ${}^4_{\Lambda}\text{H}$ hypernucleus with one week beam time.

5.2 Background processes and simulation study

As described in Appendix B, most contamination come from quasi-free Λ and $\Sigma^{-,0}$ production after requesting forward π^0 and single π^- track inside CDS. To have a reliable estimation for the signal to noise ratio, we performed GEANT4 simulation directly with 1 GeV/c K^- beam bombarding liquid ${}^3\text{He}$ target. So that the GEANT4 built-in Hyperon production cross section can provide an order of magnitude estimation for the final π^- spectrum. A realistic experimental setup including all target materials has also been implemented in the current simulation. Because of the heavy computing load needed to track all the particles in GEANT4 simulation model, we artificially increased the density of liquid ${}^3\text{He}$ target by a factor of ten (from 0.081 g/cm^3 to 0.81 g/cm^3). This modification allows us to simulate one day experimental luminosity with one week computing time on a 40 CPU Linux server. The simulation data was analyzed with offline analyzer. In the offline analysis, we request γ -ray energy $\geq 600\text{ MeV}$ from calorimeter and a single minus charged CDS track with mass in-between $0.3\text{ GeV}/c^2$

and $0.05 \text{ GeV}/c^2$.² From the simulation, we also found that the trigger rate is $\sim 100 \text{ Hz}$ by requesting forward γ -ray events and $\text{CDH} \geq 1$ hit.

The π^- spectrum survived all event selection conditions are shown in Fig.12.³ Different from the stopped-K experiment in [8], we found from the simulation that the contamination from prompt reaction is not so serious. If this is the case, there is no need to select the delayed events and the whole event sample can be used to derive the lifetime.

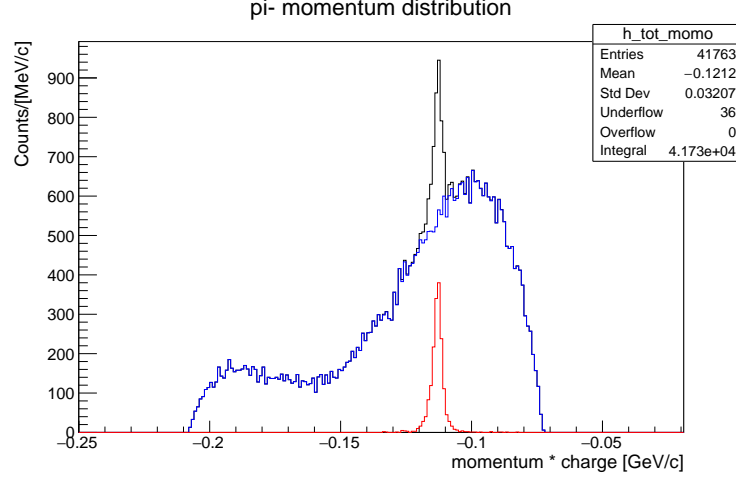


Figure 12: π^- momentum distribution: peak in red is from ${}^3_{\Lambda}\text{H}$ decay, blue curve shows π^- from other hyperon weak decay channels based on GEANT4 simulation.

5.3 Analysis procedure

Similar to [8], the first step of the data analysis is to select π^- decayed from ${}^3,4_{\Lambda}\text{H}$ based on Fig.12. In this example for ${}^3_{\Lambda}\text{H}$, we have set signal region in between $111 \text{ MeV}/c$ and $116 \text{ MeV}/c$; lower background region as $108.5 \text{ MeV}/c \sim 111 \text{ MeV}/c$; higher background region as $116 \text{ MeV}/c \sim 118.5 \text{ MeV}/c$. By subtracting the background π^- time distribution from the event region, the time distribution related to ${}^3_{\Lambda}\text{H}$ is obtained in Fig.13, where ${}^3_{\Lambda}\text{H}$ lifetime has been assumed to be $\sim 200 \text{ ps}$.

The relation of ${}^3,4_{\Lambda}\text{H}$ lifetime and measured timing information is illustrated in Fig.7. The experimental accessible information is $T_{\text{CDH}} - T_0$, which is composed of t_{beam} , t_{π^-} and τ_0 as

$$T_{\text{CDH}} - T_0 = t_{\text{beam}} + t_{\pi^-} + \tau_0. \quad (1)$$

The value of t_{beam} and t_{π^-} can be calculated by CDS tracking⁴. The τ_0 is not the *exact* lifetime of ${}^3_{\Lambda}\text{H}$ but the lifetime convoluted with CDS time resolution, which can be written as:

$$f(t) = \int_{-\infty}^{+\infty} e^{-(t-u)/\tau} R(u) du, \quad (2)$$

²The mass calculated as the TOF between reaction vertex and CDH hit position doesn't include the weak decay lifetime effect. Therefore, the calculated mass is shifted to the heavier side by $\sim 50 \text{ MeV}/c^2$. As far as the PID can separate π^- from K^- , this mass shift will not cause serious problem in the energy loss correction and event selection.

³The background events from hyperon decay are scaled by a factor of two in order to tolerate the ambiguity in GEANT4 simulation. As one can see, the S/N is still in an acceptable level even after scaling.

⁴For details of vertex reconstruction and velocity derivation with CDS, please refer to [12].

where $R(u)$ is the response function due to limited time resolution. By assuming $R(u)$ as a Gaussian function with $\sigma = 200$ ps, which is the current CDS time resolution, the ${}^3\Lambda$ lifetime can be derived by fitting the π^- time spectrum with $f(t)$. Qualitatively, one can estimate the achievable lifetime resolution by calculating its *standard deviation of the mean* as the order of a few ten ps. A quick fitting gives a reasonable resolution of ~ 40 ps.

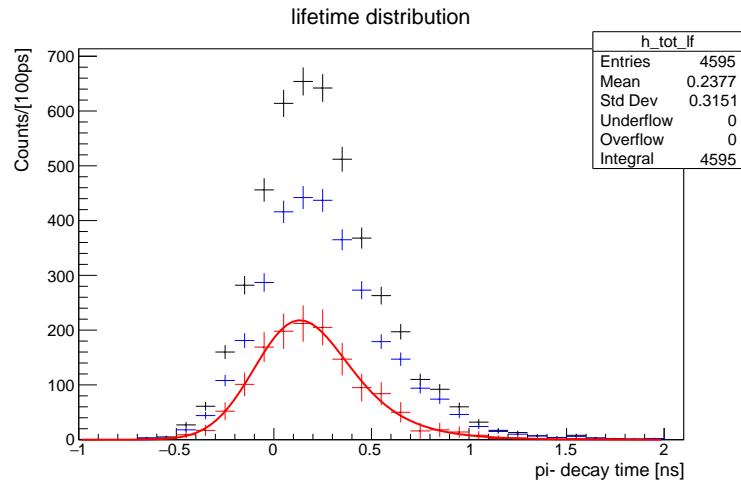


Figure 13: Time distribution of π^- after event selection: blue data points are background events from hyperon decay; red data points are ${}^3\Lambda$ events after subtracting background distribution.

6 Proposal timeline

6.1 Liquid ^3He target modification

The current E15 target system uses a large cylindrical vacuum chamber, which conflicts with the proposed PbF_2 calorimeter installation position. We have to modify the current design with a thinner vacuum pipe to allocate space for the calorimeter. There are feasible design experience from J-PARC E13 collaboration for us to follow. In principle, target modification can be finished in one year from now. The remaining ^3He purchased for E15 experiment can be used for our measurement.

6.2 PbF_2 calorimeter construction and commissioning

We will receive 30 pieces of PbF_2 crystals from SIC, CAS, Shanghai, China in this autumn(2018). We will assemble the crystals to construct γ -ray calorimeter and test its performance in winter at ELPH of Tohoku University with gamma-ray beam. The gain of the photon sensors will be studied and aligned with the test beam.

One of the possible challenges we need to verify is the particle flux into CDC due to the installation of PbF_2 calorimeter, which has a rather high density (7.7 g/cm^3). If there are too many CDC hits caused by δ -ray and γ -ray emitted from the calorimeter, the safe operation of CDC will become a problem. The simulation result with $1 \times 10^6 \text{ K}^-$ beam is shown in Fig.14. It seems that the CDC flux will only increase slightly if we install calorimeter at 70 cm from target center, which is represented by red curve in Fig.14. However, we need to verify the feasibility of this setup in the beginning of the beam time.

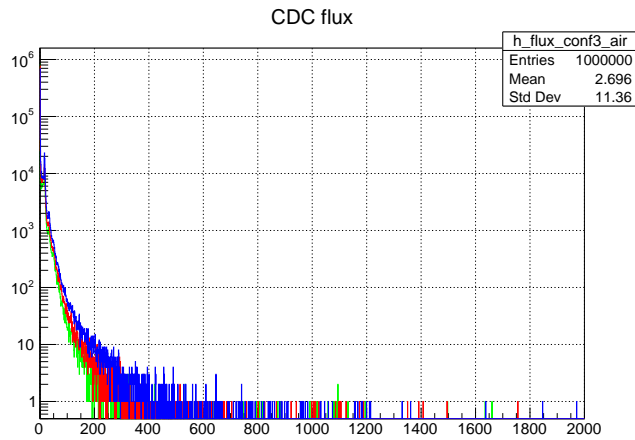


Figure 14: CDC hits flux distribution per event with different detector setup: W/O PbF_2 calorimeter (green), PbF_2 calorimeter located at 70 cm downstream of target center (red), PbF_2 calorimeter located at 30 cm of target center (blue).

7 Beam time request

Based on the estimation described in the previous sections, we require in total 38 days beam time with 50 kW beam power. The details for the beam time schedule is listed as:

Detector commissioning	:	3 days
${}^4_{\Lambda}\text{H}$ production	:	7 days
${}^3_{\Lambda}\text{H}$ production	:	28 days

References

- [1] M. Juric *et al.*, Nucl. Phys. B, **52**, 1, (1973)
- [2] Private communication with Prof. E. Hiyama, (2016)
- [3] L. Adamczyk *et al.*, Phys. Rev. C, **97**, 054909, (2018)
- [4] C. Rappold *et al.*, Nucl. Phys. A, **913**, 170, (2013)
- [5] ALICE collaboration, Phys. Lett. B, **754**, 360, (2016)
- [6] M. Block *et al.*, Proc. Int. Conf. Hyperfragments, 63, (1963)
- [7] H. Bhang *et al.*, J. Kor. Phys. Soc., **59**, 1461, (2011)
- [8] H. Ota *et al.*, Nucl. Phys. A, **547**, 109c, (1992)
- [9] Private communication with Dr. F. Sakuma, (2016)
- [10] G. Armenteros *et al.*, Nucl. Phys. B, **8**, 233, (2012)
- [11] Private communication with Prof. T. Harada, (2016)
- [12] K. Agari *et al.*, Prog. Theo. Exp. Phys., **02B011**, (2012)
- [13] D.F. Anderson *et al.*, Nucl. Inst. Meth. A, **290**, 385, (1990)
- [14] T. Hashimoto, Doctor Thesis, University of Tokyo, (2013)
- [15] www.srim.org

A ${}^3_{\Lambda}\text{H}$ stopping time estimation

The recoiling ${}^3_{\Lambda}\text{H}$ gradually stops inside liquid ${}^3\text{He}$ target before it decays. The stopping power in [MeV/mm] units for different kinetic energy of ${}^3_{\Lambda}\text{H}$ is given in Fig.15 based on calculation with *SRIM*[?]. The stopping power in Fig.15 is fitted with a 4th order polynomial. This curve can be converted into stopping time and recoil momentum relation. The results is shown in Fig.16. We can read from Fig.16 that the ${}^3_{\Lambda}\text{H}$ with $p \leq 0.2$ GeV/c ($p \leq 0.3$ GeV/c) recoiling momentum will be stopped after ~ 150 ps (~ 400 ps). It implies that by selecting π^- event with long enough delay, the ${}^3_{\Lambda}\text{H}$ hypernucleus is effectively decay at rest.

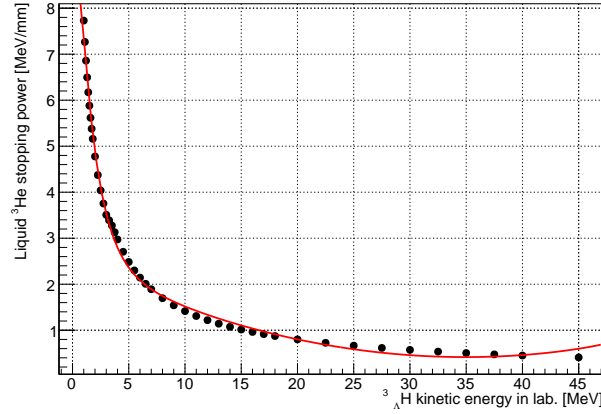


Figure 15: Stopping power of liquid ${}^3\text{He}$ target for recoiling ${}^3_{\Lambda}\text{H}$ hypernucleus.

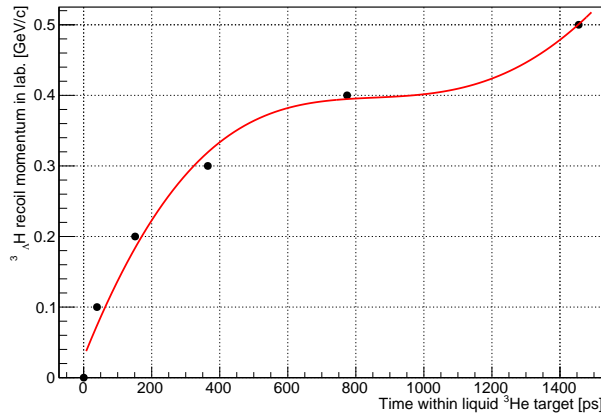


Figure 16: Slowing down of recoiling ${}^3_{\Lambda}\text{H}$ hypernucleus within liquid ${}^3\text{He}$ target as a function of time.

B Background Survey

The survey for K^- related reaction channels as possible background are listed in Table 4[10]. The reactions involve a prompt π^- can be effectively suppressed by selecting delayed events[8]. Most con-

tamination after selecting fast π^0 and delayed π^- comes from quasi-free Λ and Σ^- production, which is used in this proposal to give a performance estimation.

Reaction(decay) and final states	Charged particle timing structure	Branching ratio	σ [mb/Sr] for $p_{K^-}=0.9$ GeV/c and $\theta_{\pi^0}=0$
$K^- \ ^3\text{He} \rightarrow \pi^0 \ ^3\text{H} \rightarrow \begin{cases} \pi^0 \pi^- \ ^3\text{He} \rightarrow 2\gamma \pi^- \ ^3\text{He} \\ \pi^0 \text{p n n}_s \rightarrow 2\gamma \text{p n n} \end{cases}$	delayed π^- delayed p	?% ?%	?% ?%
$K^- \rightarrow \begin{cases} \pi^0 \mu^- \bar{\nu}_\mu \rightarrow 2\gamma \mu^- \bar{\nu}_\mu \\ \pi^0 \pi^- \rightarrow 2\gamma \pi^- \\ \pi^0 \pi^0 \pi^- \rightarrow 4\gamma \pi^- \end{cases}$	prompt μ^- prompt π^- prompt π^-	3.32% 20.92% 1.76%	Not included
$K^- \text{p} \rightarrow \pi^0 \Lambda \rightarrow \begin{cases} \pi^0 \pi^0 \text{n} \rightarrow 4\gamma \text{n} \\ \pi^0 \pi^- \text{p} \rightarrow 2\gamma \pi^- \text{p} \end{cases}$	N. A. delayed π^- , p	35.8% 63.9%	4.5
$K^- \text{p} \rightarrow \pi^0 \Sigma^0 \rightarrow \pi^0 \gamma \Lambda \rightarrow \begin{cases} \pi^0 \gamma \pi^0 \text{n} \rightarrow 5\gamma \text{n} \\ \pi^0 \gamma \pi^- \text{p} \rightarrow 3\gamma \pi^- \text{p} \end{cases}$	N. A. delayed π^- , p	35.8% 63.9%	0.36 (scaled)
$K^- \text{p} \rightarrow \pi^- \Sigma^+ \rightarrow \begin{cases} \pi^- \pi^0 \text{p} \rightarrow 2\gamma \pi^- \text{p} \\ \pi^- \pi^+ \text{n} \end{cases}$	prompt π^- , delayed p N. A.	51.57% 48.31%	0.9
$K^- \text{p} \rightarrow \pi^+ \Sigma^- \rightarrow \pi^+ \pi^- \text{n}$	N. A.	100%	Not included
$K^- \text{n} \rightarrow \pi^- \Lambda \rightarrow \begin{cases} \pi^- \pi^0 \text{n} \rightarrow 2\gamma \pi^- \text{n} \\ \pi^- \pi^- \text{p} \rightarrow 2\pi^- \text{p} \end{cases}$	prompt π^- N. A.	35.8% 63.9%	Not included
$K^- \text{n} \rightarrow \pi^- \Sigma^0 \rightarrow \pi^- \gamma \Lambda \rightarrow \begin{cases} \pi^- \gamma \pi^0 \text{n} \rightarrow 3\gamma \pi^- \text{n} \\ \pi^- \gamma \pi^- \text{p} \rightarrow \gamma 2\pi^- \text{p} \end{cases}$	prompt π^- N. A.	35.8% 63.9%	Not included
$K^- \text{n} \rightarrow \pi^0 \Sigma^- \rightarrow \pi^0 \pi^- \text{n} \rightarrow 2\gamma \pi^- \text{n}$	delayed π^-	100%	0.9 (scaled)

Table 4: Survey for $K^- + \ ^3\text{He} \rightarrow$ forward π^0 + delayed π^- .